# नाभिकीय अभिक्रिया

4

## दुर्बल-बंध स्थिर नाभिक से जुड़े अभिक्रिया तंत्र को उजागर करना

**एस.के. पंडित[1,2,*], ए.के. श्रीवास्तव[1,2], के. माहात[1,2], के. रामचंद्रन[1] और पी.सी. राउत[1,2]**
[1]नाभिकीय भौतिकी प्रभाग, भाभा परमाणु अनुसंधान केंद्र (भापअ केंद्र), ट्रांबे, मुंबई – 400085, भारत
[2]होमी भाभा राष्ट्रीय संस्थान, अणुशक्तिनगर, मुंबई – 400094, भारत

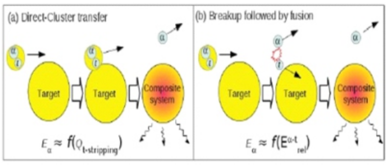


*$^{7}$Li (α+ t) + लक्षित अभिक्रिया हेतु समूह के विभंजन में से एक के संलयन के बाद (a) प्रत्यक्ष-समूह हस्तांतरण और (b) विभाजन को दर्शाने वाला चित्रण।*

सारांश

कण-कण और कण-γ-किरण संयोग माप का उपयोग करके $^{7}$Li (α+ t) + $^{93}$Nb प्रणाली के लिए दुर्बल-बंध में स्थिर नाभिक से जुड़े अभिक्रिया तंत्र की जांच की गई। विभिन्न विघटन अभिक्रिया चैनलों को समझने के लिए कण-कण संयोग माप किया गया, जबकि कण-γ-किरण संयोग माप का उपयोग बड़े α कण उत्पादन और अपूर्ण संलयन अभिक्रिया चैनलों की उत्पत्ति को समझने के लिए किया जाता है। टी-कैप्चर तंत्र को ~ 70% प्रभावित करता पाया गया। गतिज स्थितियों के उचित चयन ने पहली बार क्षेत्र की एक महत्वपूर्ण आबादी को केवल प्रत्यक्ष ट्राइटन स्ट्रिपिंग प्रक्रिया के लिए सुलभ होने की अनुमति दी और इसके बाद "मुक्त" ट्राइटन (त्रि-निकाय निरंतरता से) पर नियंत्रण के बाद विभंजन की अनुमति नहीं दी। यह परिणाम, स्पष्ट रूप से बड़े अल्फा उत्पादन में प्रत्यक्ष क्लस्टर-स्ट्रिपिंग तंत्र के प्रभुत्व को स्थापित करता है।

# Nuclear Reactions

4

## Unravelling the Reaction Mechanisms involving Weakly-bound Stable Nuclei

**S. K. Pandit[1,2,*], A. K. Shrivastava[1,2], K. Mahata[1,2], V. V. Parkar[1,2], K. Ramachandran[1] and P. C. Rout[1,2]**
[1]Nuclear Physics Division, Bhabha Atomic Research Centre (BARC), Trombay, Mumbai-400085, INDIA
[2]Homi Bhabha National Institute, Anushakti Nagar, Mumbai-400094, INDIA

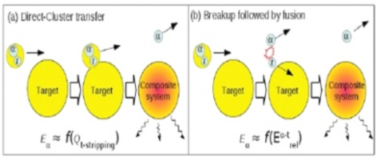


*Illustration depicting (a) direct-cluster transfer and (b) breakup followed by fusion of one of the cluster fragments for $^{7}$Li(α+t)+target reaction.*

ABSTRACT

The reaction mechanisms involving weakly bound stable nuclei has been investigated using particle-particle and particle-γ-ray coincidence measurements for $^{7}$Li(α+t)+$^{93}$Nb system. Particle-particle coincidence measurements were carried out to understand various breakup reaction channels, while particle-γ-ray coincidence measurements is utilised to understand the origin of the large α particle production and incomplete fusion reactions channels. The t-capture mechanism is found to be dominant ~70%. Proper choice of kinematical conditions allowed for the first time a significant population of the region accessible only to the direct triton stripping process and not to breakup followed by the capture of the “free” triton (from the three-body continuum). This result, clearly establishes the dominance of the direct cluster-stripping mechanism in the large alpha production.

KEYWORDS: *Direct nuclear reaction, weakly bound nuclei, fusion, cluster in nuclei*

**Author for Correspondence: S. K. Pandit*
*E-mail: sanat@barc.gov.in*

### Introduction

Exploring the properties of weakly bound stable and unstable nuclei with α+x cluster structure, e.g., $^{6,8}$He, $^{6,7}$Li, and $^{7,9}$Be, is a topic of current interest [1,2] and also a focus of the next generation of high intensity isotope-separation online (ISOL) radioactive ion beam facilities. Apart from elastic scattering and fusion, due to the low breakup threshold of such nuclei, the population of the continuum is probable and consequently a large coupling effect is expected at energies around the Coulomb barrier. This may take place directly through inelastic excitation of the projectile (prompt or resonant breakup) or by nucleon transfer leaving the ejectile in an unbound state (transfer breakup) [1–15]. Another reaction channel, breakup followed by capture of fragments (only part of the projectile fuses) known as incomplete fusion is an important reaction and interestingly it is dominant over fusion at energies below the Coulomb barrier.

The origin of the observed large inclusive α-particle production cross sections compared to that of the complementary fragments is also important to understand. Different reaction mechanisms, e.g., breakup (direct and sequential), nucleon transfer followed by breakup, cluster transfer, incomplete fusion and compound nuclear (CN) evaporation, contribute to the α-yield.

It is difficult to separate the contributions of these individual reaction mechanisms from an inclusive measurement. Exclusive measurements are therefore needed to disentangle the different reaction processes, discussed above. In this investigation, we aimed to disentangle different reaction channels utilising exclusive measurements and quantum mechanical coupled channels calculations.

### Experimental Details

All the measurements were carried out at the Pelletron-Linac facility, Mumbai, with $^7$Li beams of 24, 26, 28, and 30 MeV. A self-supporting $^{93}$Nb foil of thickness ~1.75 mg/cm$^2$ was used as a target. For the measurements of breakup reaction channels, the requirements of high granularity to detect low-lying resonant states and large solid angle to measure low cross-section events were achieved using segmented large area Si telescopes of active area 5 × 5 cm$^2$. The ΔE-detectors (50 μm thick) were single-sided and the E-detectors (1.5 mm thick) were double-sided with 16 strips allowing a maximum of 256 pixels. Two such telescopes, set 30◦ apart, were mounted at a distance of 16 cm from the target on a movable arm in a scattering chamber. In this geometry, the cone angle between the two detected fragments ranged from 1$^0$ to 24$^0$. The angular range 30$^0$–130$^0$ (around the grazing angle) was covered by measurements at different angle settings. Three Si surface barrier detector telescopes (thicknesses: ΔE ~ (20-50 μm, E ~ 450–1000 μm) were used to obtain the elastic scattering angular distribution at forward angles (25$^0$–40$^0$) where the count rate is too high for the strip detectors to cope with. Two Si surface-barrier detectors (thickness ~300 μm) were kept at ±20$^0$ for absolute normalization. The detectors were calibrated using the known α energies from a $^{239}$Pu-$^{241}$Am source and the $^7$Li+$^{12}$C reaction at 24 MeV. Breakup fragments in coincidence were measured at beam energies of 24, 28, and 30 MeV.

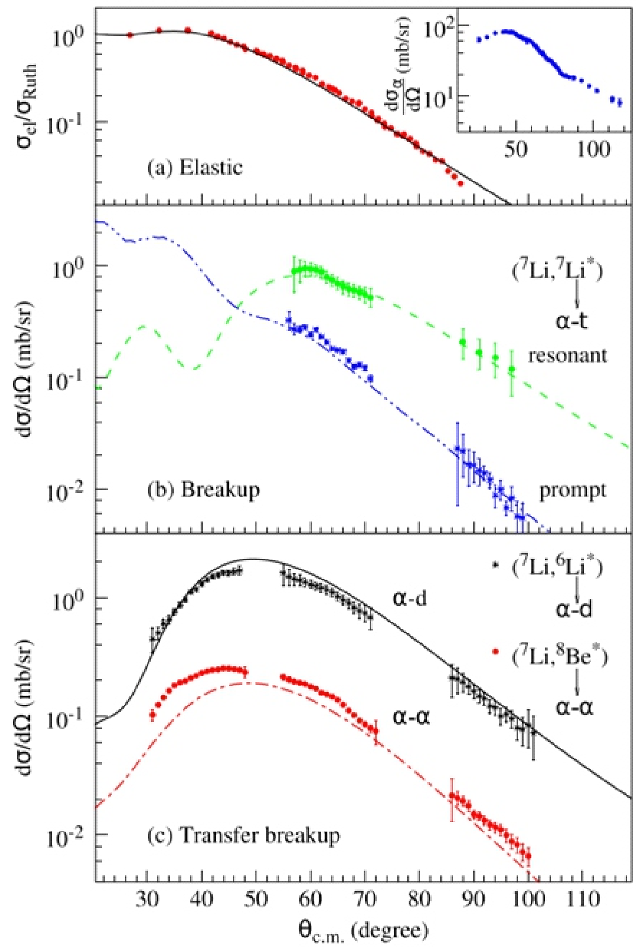


*Fig.1: Measured inclusive and exclusive cross sections for the $^7$Li+$^{93}$Nb system at 28 MeV. (a) Elastic scattering data and the CDCC calculation. The inclusive cross section for α production is shown in the inset. (b) Prompt and resonant (from the 7/2$^-$ state) breakup of $^7$Li, shown as asterisks and filled circles, respectively.*

Two independent experiments were carried out for in-beam and off-beam γ-ray counting. Both the measurements were performed at beam energies of 24, 26, 28, and 30 MeV, some of which are common to the exclusive measurement of breakup fragments.

Prompt γ-ray transitions were detected using the Indian National Gamma Array (INGA) [16], consisting of 18 Compton suppressed high purity germanium (HPGe) clover detectors. In this particular array configuration, the detectors were arranged at six different angles with three detectors each at ±40$^0$, −65$^0$, and −23$^0$, two detectors at +65$^0$ and four detectors at 90$^0$. Three Si surface barrier telescopes (thicknesses: ΔE ~15−30 μm, E ~ 300−5000μm), were placed inside the scattering chamber at 35$^0$, 45$^0$, and 70$^0$ for the detection of charged particles around the grazing angle. One Si surface barrier detector (thickness ~300 μm) was fixed at 20$^0$ to monitor Rutherford scattering for absolute normalization purposes. The time stamped data were collected using a digital data acquisition system with a sampling rate of 100 MHz [16]. Efficiency and energy calibration of the clover detectors were carried out using standard calibrated $^{152}$Eu and $^{133}$Ba γ-ray sources.

The off-line γ-ray counting was carried out using an efficiency calibrated high-purity germanium (HPGe) detector. Low background was achieved by using graded shielding (Cu, Cd sheets of thickness ~2 mm each followed by 5 cm of Pb). Aluminum catcher foils of thickness ~1 mg/cm$^2$ were used together with each target foil to stop the recoiling residues. The target and catcher foil assemblies were irradiated for ~6 h (beam current ~50 nA) at each bombarding energy and counted together at a distance of 10 cm from the detector. A CAMAC scaler which recorded the integrated current in intervals of 1 min duration was used to monitor beam current.

### Data Analysis and Results (A)

Detected particles were identified from energy loss information and tagged by kinetic energy (E), identity (A, Z), and scattering angle (θ, φ) with respect to the beam axis. The relative angles ($\theta_{rel}$) between the fragments were calculated from the measured scattering angles ($\theta_1$, $\varphi_1$; $\theta_2$, $\varphi_2$). The fragments' mass, kinetic energy ($E_1$, $E_2$), and $\theta_{rel}$ were used to calculate their relative energy ($E_{rel}$). The excitation energy of the ejectile prior to breakup was obtained by adding the breakup threshold to the measured $E_{rel}$. The $E_{rel}$ spectra for α+α, α+d, and α+t exhibit peaks at 0.092, 0.71, and 2.16 MeV that correspond to the breakup of $^8$Be (g.s.), $^6$Li (2.18 MeV, $3^+$), and $^7$Li (4.63 MeV, $7/2^-$), respectively.

The excitation energy of the target-like nuclei was determined using the missing energy technique. For the transfer reactions, this was found to peak around the energy $E^*=Q_{gg}-Q_{opt}$, as expected from the semi classical theory of trajectory matching [17]. Here $Q_{gg}$ and $Q_{opt}$ are the ground state and optimum Q values, respectively.

The efficiency for the detection of fragments in coincidence was estimated using the Monte Carlo technique, taking into account the excitation of the target as well as the ejectile, the Q value of the reaction, the energy resolution, and detection threshold. The efficiency depends on the velocity of the ejectile prior to breakup as well as the relative velocity of the fragments [18,19]. The scattering angle of the ejectile prior to breakup was assumed to be isotropic. The scattered energy of the ejectile was calculated using kinematics. The breakup fragment emission in the rest frame of the ejectile was also considered to be isotropic. The velocities of each fragment in the rest frame of the ejectile were calculated using energy and momentum conservation laws. These velocities were added to the velocity of the ejectile prior to breakup to get their velocities in the laboratory frame. It was checked whether both fragments hit two different vertical and horizontal strips. Events satisfying this condition were considered as detectable events for estimation of the efficiency. The conversion of the energy and scattering angle from the laboratory frame to the c.m. frame of the target-projectile in event-by-event mode automatically takes care of the Jacobian of the transformation.

The angular distributions of elastic scattering, projectile breakup, and transfer followed by breakup for the $^7$Li+$^{93}$Nb system at 28 MeV are shown in Fig.1. The elastic scattering data are presented in Fig.1(a). The errors on the data points are due to statistics. The $^7$Li*→ α + t breakup via the $7/2^-$ state and the continuum below this resonance are shown in Fig.1(b). The cross sections for 1p pickup leading to the $^8$Be(g.s.) are shown in Fig.2(c). These data are restricted to $^{92}$Zr excitation energies up to 3.0 MeV, as information on the spectroscopic factors is available only in this energy range. For 1n stripping, the cross sections for α + d breakup events from the $^6$Li $3^+$ (2.18 MeV) state are shown in Fig.2(c). Excited states of 94Nb up to 1.0 MeV were considered. The differential cross sections for α+d events from the breakup of $^6$Li formed after 1n stripping are larger than those for α+t events from the resonant breakup of $^7$Li, while those for α+α events due to 1p pickup forming $^8$Be are smaller [20, 21].

### Data Analysis and Results (B)

The residues populated by t-capture, complete fusion (CF), and nucleon(s)-transfer identified by detecting their characteristic γ-rays. The α-particle gated γ-ray spectrum, were obtained, which shows the major reaction processes contributing to the α-particle yield. The relative yields of γ-ray transitions from the residues of t- capture ($^{94,95}$Mo) are found to be greater than the others. The other reaction mechanisms contributing to the α yields, namely, 1p pickup ($^7$Li,$^8$Be → α + α)$^{92}$Zr, inelastic excitation ($^7$Li,$^7$Li* → α + t)$^{93}$Nb, 1n stripping ($^7$Li,$^6$Li* → α + d)$^{94}$Nb, and 2n-stripping ($^7$Li,$^5$Li → α+p)$^{95}$Nb were also identified.

The cross sections for the residues from the t-capture mechanism, $^{94,95}$Mo, were extracted. For $^{94}$Mo, the yrast γ-ray transitions built on the ground state up to the $J^\pi = 10^+$ excited state was considered. The cross sections for 95Mo were obtained by adding the γ-ray transitions feeding directly to the ground state. The $^{93}$Mo nucleus has a $21/2^+$ isomeric state at $E_{ex}$ =2.425 MeV with half-life $T_{1/2}$ = 6.85 h. The cross section for $^{93m}$Mo was obtained by following the radioactive decay of the isomeric state. The uncertainty in the measured cross sections were estimated considering (1) statistics, (2) γ-ray detection efficiency, and (3) available spectroscopic information of the residues. For off-beam measurements uncertainty in the target thickness was also included.

The α-capture and 2n-stripping mechanisms lead to $^{95,96}$Tc and $^{95}$Nb. These nuclei are radioactive with reasonable half-

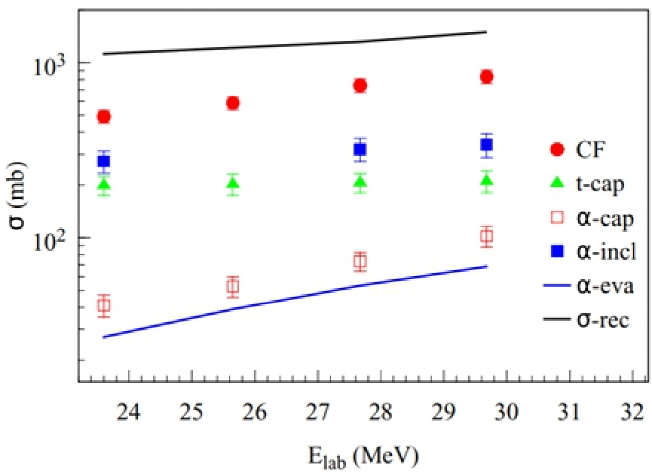


*Fig.2: The measured cross sections for t-capture, α-capture, CF, inclusive-α are denoted by filled triangles, open squares, filled circles, and filled squares, respectively. The blue line is the estimated α-evaporation cross section from the statistical model calculations. The calculated reaction cross sections are also shown by the black line.*

lives for decay from their ground states [$T_{1/2}$($^{95}$Tc) = 20.0 h, $T_{1/2}$($^{96}$Tc) = 4.28 d, $T_{1/2}$($^{95}$Nb) = 34.99 d] as well as from metastable states [$T_{1/2}$($^{95}$Tc) = 61 d, $T_{1/2}$($^{96}$Tc) = 51.5 m, $T_{1/2}$($^{95}$Nb) = 3.61 d]. The γ-ray transitions corresponding to decay of $^{95,96}$Tc and $^{95}$Nb were identified. The cross sections were extracted following the half-lives of each transition. The complete fusion of $^{7}$Li with $^{93}$Nb forms the compound nucleus (CN) $^{100}$Ru, which decays predominantly by neutron and proton emission. The characteristic prompt γ-ray transitions of the evaporation residues (ERs) $^{96-98}$Ru and $^{97}$Tc were also identified. The cross sections of $^{96-98}$Ru and $^{97}$Tc were obtained using the in-beam method. The cross sections for $^{97}$Ru were also extracted using the off-beam γ-ray counting method and found to be consistent with the in-beam measurements and with the values reported in Ref. [22].

The cross sections of individual residues from α and t-capture were corrected for the contribution from the compound nucleus. The t-capture, α-capture, and complete fusion cross sections were obtained by taking the sum of individual residue cross sections and are presented in Fig.2 [23]. The cross sections for t-capture are found to be larger than those for α-capture at all energies, in agreement with the results reported in earlier studies with $^{7}$Li projectiles [24-26]. The estimated α-particle evaporation and the extracted reaction cross sections are also plotted in Fig.3.

The t-capture reaction can arise due to either direct stripping of a cluster from a bound state of the projectile or fusion of one of the "free" fragments after breakup of the projectile, i.e., so called breakup-fusion [23]. These two mechanisms were disentangled by proper kinematic conditions. The α-particle energy spectrum at 35$^{0}$ gated with the characteristic γ-rays of $^{94,95}$Mo shows a substantial

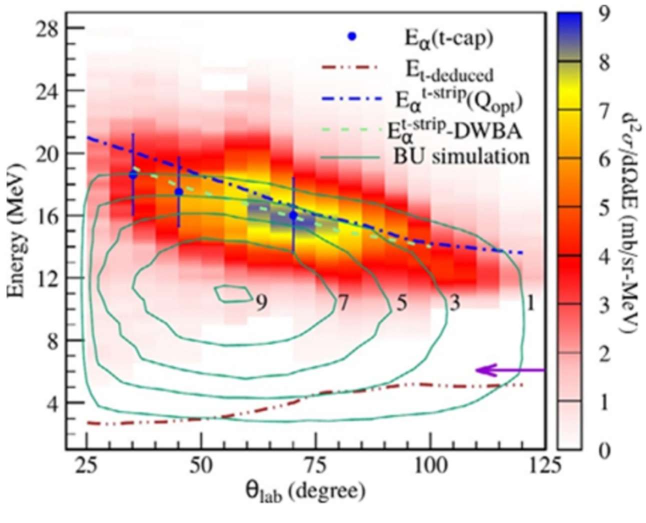


*Fig.3: Measured energy-angle correlation spectrum of inclusive α particles in the $^{7}$Li+$^{93}$Nb reaction compared with the kinematical line for $Q_{opt}$ (dot-dashed line) and the DWBA calculations (dashed line) for t stripping. Mean values of the measured α-energy at three different laboratory angles in coincidence with prompt γ rays are shown as filled circles along with the width (FWHM). The results of a breakup simulation are shown as contours (see text for details). The energy of the triton calculated from the mean energy of the inclusive α spectra assuming breakup followed by capture of a triton by the target is shown by the dot-dot-dashed line. The arrow indicates the position of the Coulomb barrier between the triton and $^{93}$Nb.*

population of $E_\alpha$ >20.5 MeV. From Q-value arguments of free-t-fusion, the α-particles ($E_\alpha$ >20.5) must be exclusively due to direct t-cluster stripping from bound states of $^{7}$Li to bound states (with respect to triton emission) of 96Mo, allowing us to put a lower limit of ~30% on this contribution [27].

The energy-angle correlations of the α-particles were analyzed for further investigation. The experimental correlations obtained from the inclusive and exclusive measurements are compared with those estimated as due to direct stripping and breakup in Fig.3. The measured inclusive and exclusive correlations exhibit similar characteristics. While the experimental correlations are in good agreement with both the kinematical curve using the optimum Q-value and DWBA calculations for t-stripping over a wide angular range (25$^{0}$-125$^{0}$), the result of the breakup simulation has very different characteristics. This further demonstrates that breakup does not make a significant contribution to the α-particle production and ICF. The energy of the triton ($E_t$) deduced from the measured mean values of $E_\alpha$ assuming the α-t breakup mechanism is found to be less than the Coulomb barrier between the t-fragment and $^{93}$Nb (indicated by the arrow) over the whole angular range. This also indicates that, due to the fusion barrier, breakup followed by fusion of the triton is very unlikely. This systematic investigation establishes the dominance of cluster stripping over breakup-fusion as the main source for the large α-yields and ICF.

## Summary and Conclusion

In summary, the present work reports for the first time a detailed study of the various breakup mechanisms, 1p pickup and 1n stripping to unbound states of the ejectile and direct breakup, for the same system at energies close to the Coulomb barrier. The absolute cross sections for t-capture, α-capture, and 2n stripping along with the complete fusion were also measured using the in-beam and off-beam γ-ray counting methods. The present study shows that the t-capture mechanism is the dominant reaction channel for the production of α particles and accounts for 62−73% of the measured inclusive α cross sections. The 2n stripping ($^{5}$Li → α + p) cross sections together with earlier data on the 1p pickup ($^{8}$Be → α + α), inelastic excitation ($^{7}$Li* → α + t), and 1n stripping ($^{6}$Li* → α + d) explain ~ 15% of the inclusive α cross sections. The statistical model predictions of the compound nuclear contributions from α-evaporation account for 10−20% of the inclusive α cross sections. With proper choice of kinematical conditions, it has been possible for the first time to populate with significant strength the part of the spectrum accessible to triton cluster stripping only and not to breakup. This provides direct experimental evidence for the dominant role of the stripping process and also allows a meaningful comparison with theoretical models. CDCC, DWBA and CCBA calculations were performed to analyze a comprehensive data set comprising elastic scattering, direct breakup, transfer breakup and t-stripping reaction channels.

This unique comprehensive dataset offers a test-bench for further development of state-of-the-art theoretical formalisms (e.g. [28-30]) for reactions involving weakly bound stable/radioactive nuclei, which are also used to simulate nucleosynthesis.

**Acknowledgment**

We acknowledge the accelerator staff for ensuring smooth running of the machine. The help extended by P. Patale during the experiment is also acknowledged.

**References**

[1] N. Keeley, N. Alamanos, K. W. Kemper, and K. Rusek, Prog. Part. Nucl. Phys. 63, 396 (2009).

[2] L. F. Canto, P. R. S. Gomes, R. Donangelo, J. Lubian, and M. S. Hussein, Phys. Rep. 596, 1 (2015).

[3] J. L. Quebert, B. Frois, L. Marquez, G. Sousbie, R. Ost, K. ́ Bethge, and G. Gruber, Phys. Rev. Lett. 32, 1136 (1974).

[4] C. Signorini et al., Phys. Rev. C 67, 044607 (2003).

[5] A. Shrivastava, A. Navin, N. Keeley, K. Mahata, K. Ramachandran, V. Nanal, V. V. Parkar, A. Chatterjee, and S. Kailas, Phys. Lett. B 633, 463 (2006).

[6] A. Pakou et al., Phys. Lett. B 633, 691 (2006).

[7] S. Santra, V. V. Parkar, K. Ramachandran, U. K. Pal, A. Shrivastava, B. J. Roy, B. K. Nayak, A. Chatterjee, R. K. Choudhury, and S. Kailas, Phys. Lett. B 677, 139 (2009).

[8] F. A. Souza et al., Nucl. Phys. A 821, 36 (2009).

[9] D. H. Luong, M. Dasgupta, D. J. Hinde, R. du Rietz, R. Rafiei, C. J. Lin, M. Evers, and A. Diaz-Torres, Phys. Lett. B 695, 105 (2011).

[10] E. C. Simpson, K. J. Cook, D. H. Luong, S. Kalkal, I. P. Carter, M. Dasgupta, D. J. Hinde, and E. Williams, Phys. Rev. C 93, 024605 (2016).

[11] R. Rafiei, R. du Rietz, D. H. Luong, D. J. Hinde, M. Dasgupta, M. Evers, and A. Diaz-Torres, Phys. Rev. C 81, 024601 (2010).

[12] D. H. Luong, M. Dasgupta, D. J. Hinde, R. du Rietz, R. Rafiei, C. J. Lin, M. Evers, and A. Diaz-Torres, Phys. Rev. C 88, 034609 (2013).

[13] D. Martinez Heimann et al., Phys. Rev. C 89, 014615 (2014).

[14] S. P. Hu et al., Phys. Rev. C 93, 014621 (2016).

[15] O. A. Capurro, A. J. Pacheco, A. Arazi, P. F. F. Carnelli, J. O. Fernandez Niello, and D. Martinez Heimann, Nuc. Phys. A 945, 186 (2016).

[16] R. Palit, S. Saha, J. Sethi, T. Trivedi, S. Sharma, B. Naidu, S. Jadhav, R. Donthi, P. Chavan, H. Tan, and W. Hennig, Nucl. Instrum. Methods Phys. Res. A 680, 90 (2012).

[17] D. M. Brink, Phys. Lett. B 40, 37 (1972).

[18] J. E. Mason, S. B. Gazes, R. B. Roberts, and S. G. Teichmann, Phys. Rev. C 45, 2870 (1992).

[19] S. K. Pandit, K. Mahata, A. Shrivastava, V. V. Parkar, K. Ramachandran, J. Instrum. 14 (01) (2019) T01005.

[20] S. K. Pandit, A. Shrivastava, K. Mahata, N. Keeley, V. V. Parkar, P. C. Rout, K. Ramachandran, I. Martel, C. S. Palshetkar, A. Kumar, A. Chatterjee, and S. Kailas, Phys. Rev. C 93,061602(R) (2016).

[21] S. K. Pandit, A. Shrivastava, K. Mahata, V. V. Parkar, N. Keeley, P. C. Rout, K. Ramachandran, C. S. Palshetkar, I. Martel, A. Kumar, A. Chatterjee, S. Kailas, Phys. Rev. C 100, 014618 (2019).

[22] D. Kumar, M. Maiti, and S. Lahiri, Phys. Rev. C 94, 044603 (2016).

[23] S. K. Pandit, A. Shrivastava, K. Mahata, V. V. Parkar, R. Palit, N. Keeley, P.C. Rout, A. Kumar, K. Ramachandran, S. Bhattacharyya, V. Nanal, C. S. Palshetkar, T.N. Nag, S. Gupta, S. Biswas, S. Saha, J. Sethi, P. Singh, A. Chatterjee, S. Kailas, Phys.

Rev. C 96, 044616 (2017).

[24] A. Shrivastava, A. Navin, A. Diaz-Torres, V. Nanal, K. Ramachandran, M. Rejmund, S. Bhattacharyya, A. Chatterjee, S. Kailas, A. Lemasson, R. Palit, V. V. Parkar, R. Pillay, P. C. Rout, and Y. Sawant, Phys. Lett. B 718, 931 (2013).

[25] M. Dasgupta, P. R. S. Gomes, D. J. Hinde, S. B. Moraes, R. M. Anjos, A. C. Berriman, R. D. Butt, N. Carlin, J. Lubian, C. R. Morton, J. O. Newton, and A. Szanto de Toledo, Phys. Rev. C 70, 024606 (2004). [26] V. V. Parkar, V. Jha, and S. Kailas, Phys. Rev. C 94, 024609 (2016).

[27] S. K. Pandit, A. Shrivastavaa, K. Mahata, N. Keeley, V. V. Parkar, R. Palit, P. C. Rout, K. Ramachandran, A. Kumar, S. Bhattacharyyae, V. Nanal, S. Biswas, S. Saha, J. Sethi, P. Singh, S. Kailas, Phys. Lett. B 820, 136570 (2021).

[28] J. Lei, A.M. Moro, Phys. Rev. Lett. 122, 042503 (2019).

[29] J. Rangel, M. Cortes, J. Lubian, L. Canto, Phys. Lett. B 803, 135337 (2020).

[30] A. Diaz-Torres, D. J. Hinde, J. A. Tostevin, M. Dasgupta, and L. R. Gasques, Phys. Rev. Lett. 98, 152701 (2007).